

Supporting Information for

Climate-driven reduction in biomass production of the Eurasian steppe coincides with nomadic migration during the first millennium CE

Feng Chen ^{a, b, c*}, Xiaoen Zhao ^{a, b, c}, Weipeng Yue ^{a, b}, Shijie Wang ^{a, b}, Yong Zhang ^d, Youping Chen ^{b, e}, Mao Hu ^{a, b, c}, Jan Esper ^{f, g}, Ulf Büntgen ^{g, h, i}, Fredrik Charpentier Ljungqvist ^{j, k}, Amy E. Hessel ^l, Max C. A. Torbenson ^f, Yujiang Yuan ^m, Martín A. Hadad ⁿ, Fidel A. Roig ^{o, p}, Honghua Cao ^{a, b, c}, Heli Zhang ^m, Yaqun Liang ^q, Fahu Chen ^{r, s, t*}

* Corresponding authors: Feng Chen feng653@163.com

Fahu Chen fhchen@itpcas.ac.cn

a Yunnan Key Laboratory of International Rivers and Transboundary Eco-Security/Ministry of Education Key Laboratory for Transboundary Eco-Security of Southwest China, Institute of International Rivers and Eco-Security, Yunnan University, Kunming 650500, China

b State Key Laboratory of Vegetation Structure, Functions and Construction, Yunnan University, Kunming 650500, China

c Southwest United Graduate School, Kunming 650092, China

d Key Laboratory of Land Surface Pattern and Simulation, Institute of Geographic Sciences and Natural Resources Research, Chinese Academy of Sciences, Beijing 100101, China

e School of Ecology and Environmental Science, Yunnan University, Kunming 650500, China

f Department of Geography, Johannes Gutenberg University, Mainz 55099, Germany

g Global Change Research Institute, Czech Academy of Sciences, Brno 60300, Czech Republic

h Department of Geography, University of Cambridge, Cambridge CB2 3EN, United Kingdom

i Department of Geography, Faculty of Science, Masaryk University, Brno 61137, Czech Republic

j Department of History, Stockholm University, Stockholm SE-10691, Sweden

k Bolin Centre for Climate Research, Stockholm University, Stockholm SE-10691, Sweden

l Department of Geology and Geography, West Virginia University, Morgantown 26506, United States

m Key Laboratory of Tree-Ring, Physical and Chemical Research, Institute of Desert Meteorology, China Meteorological Administration, Urumqi 830002, China

n Laboratorio de Dendrocronología de Zonas Áridas-Instituto y Museo de Ciencias Naturales, Universidad Nacional de San Juan, Centro de Investigaciones de la Geósfera y Biosfera, Consejo Nacional de Investigaciones Científicas y Técnicas - Universidad Nacional de San Juan, San Juan 3306, Argentina

o Laboratorio de Dendrocronología e Historia Ambiental, Instituto Argentino de Nivología, Glaciología y Ciencias Ambientales, Consejo Nacional de Investigaciones Científicas y Técnicas-

Universidad Nacional de Cuyo, Mendoza 5500, Argentina

p Hénera Centro de Observación de La Tierra, Escuela de Ingenier ú Forestal, Facultad de Ciencias, Universidad Mayor, Huechuraba, Santiago 8580745, Chile

q School of History and Administration, Yunnan Normal University, Kunming 650500, China

r Alpine Paleoecology and Human Adaptation Group, State Key Laboratory of Tibetan Plateau Earth System, Environment and Resources, Institute of Tibetan Plateau Research, Chinese Academy of Sciences, Beijing 100101, China

s College of Resources and Environment, University of Chinese Academy of Sciences, Beijing 100049, China

t Key Laboratory of Western China's Environmental Systems (Ministry of Education), Lanzhou University, Lanzhou 730000, China

This PDF file includes:

Figures S1 to S5

Tables S1 to S3

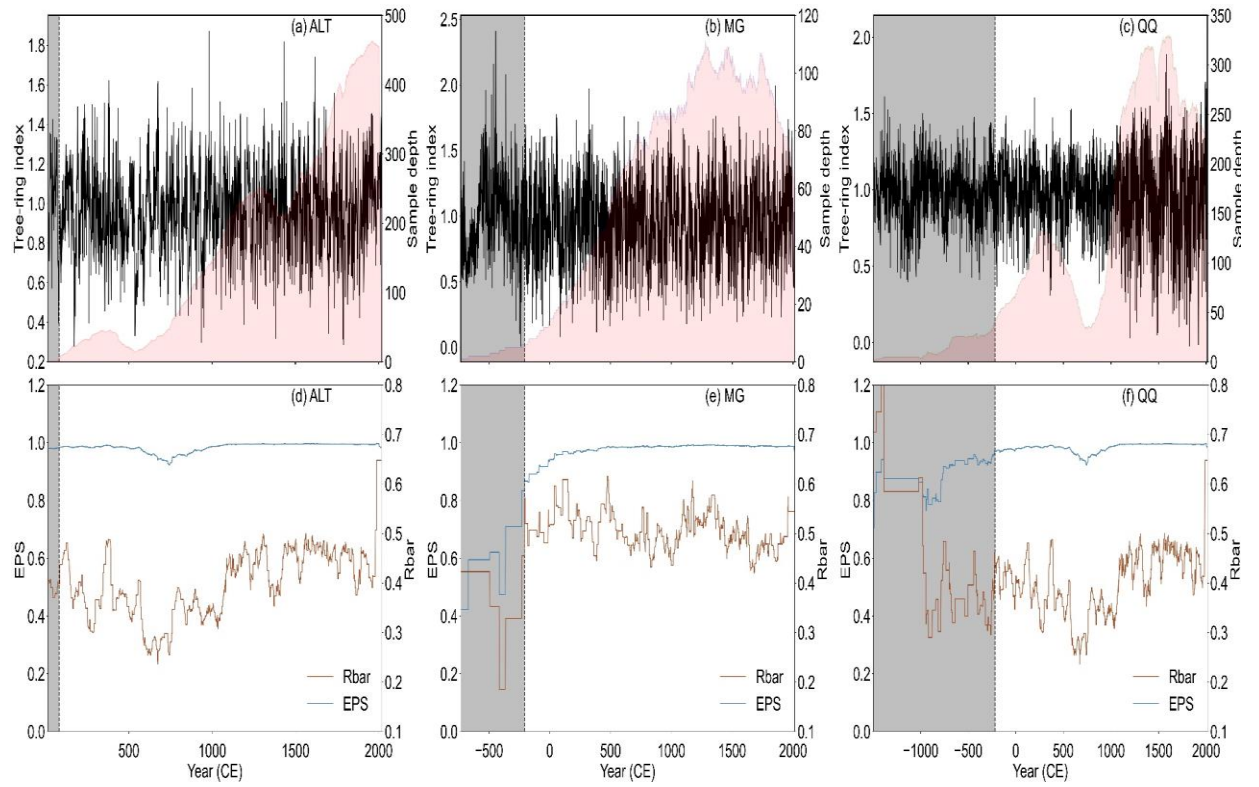


Fig. S1. (a-c) Plot of the composite chronologies (ALT, MG, QQ), and (d-f) its running expressed population signal (EPS) and the sample depth.

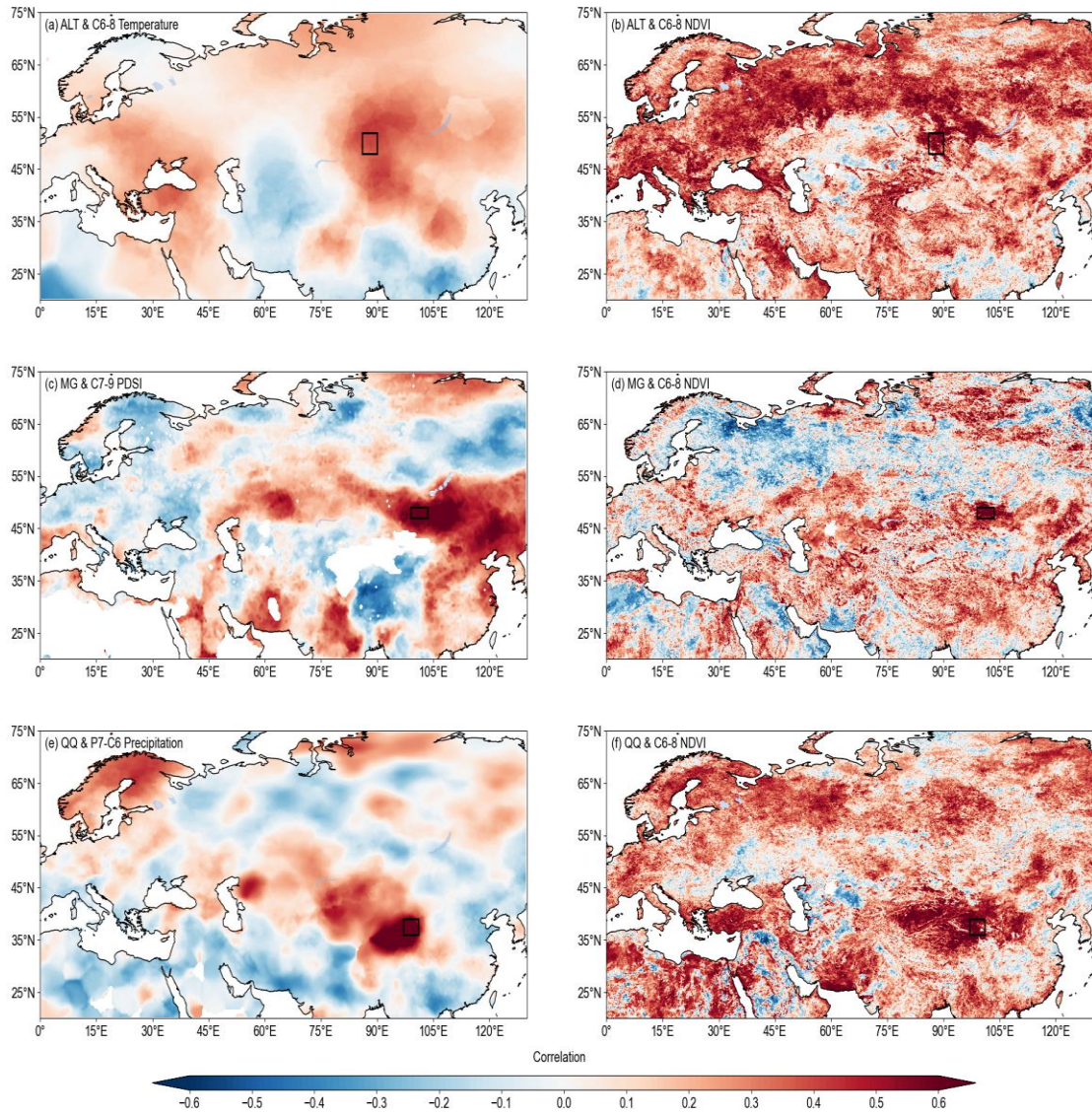


Fig. S2. (a-f) Spatial correlation patterns between the composite chronologies (ALT, MG, QQ) and climatic factors and June–August NDVI data over the common periods.

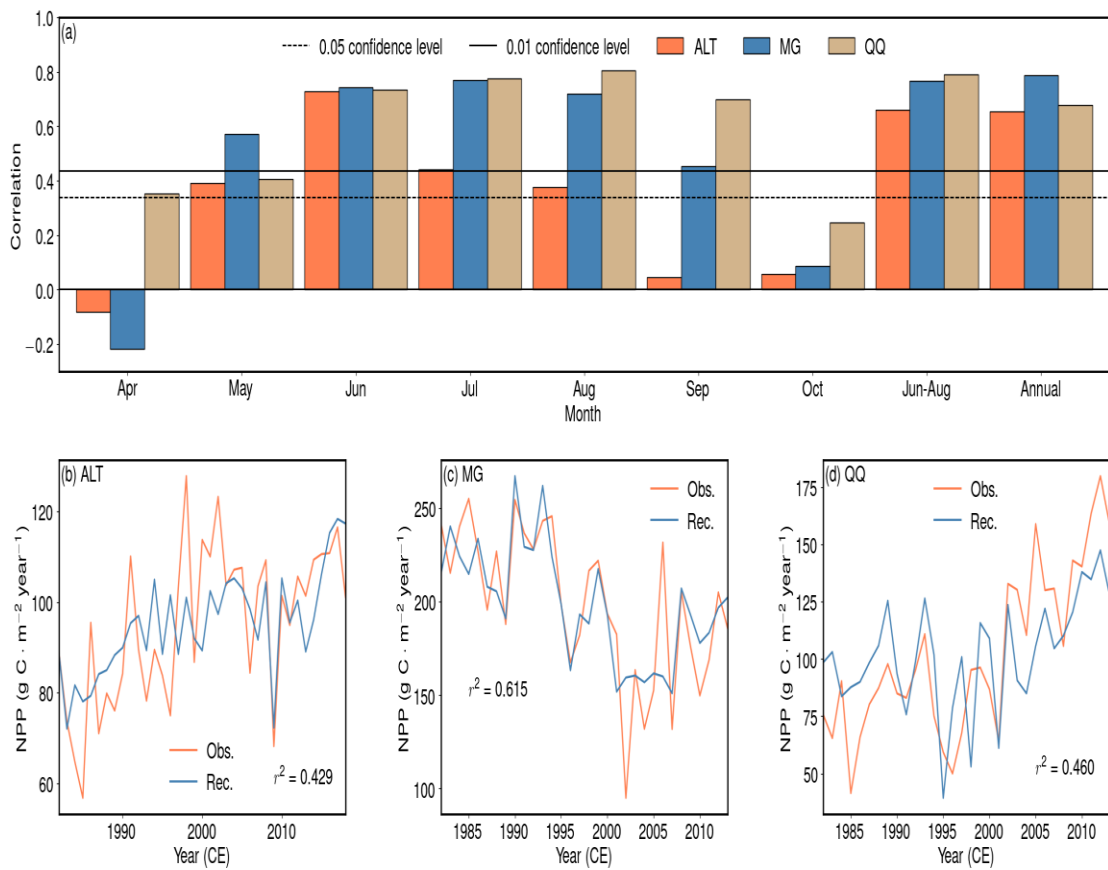


Fig. S3. (a) Correlations of the composite chronologies (ALT, MG, QQ) and monthly NPP. (b-d) Comparison of the reconstructed and observed NPP since 1982.

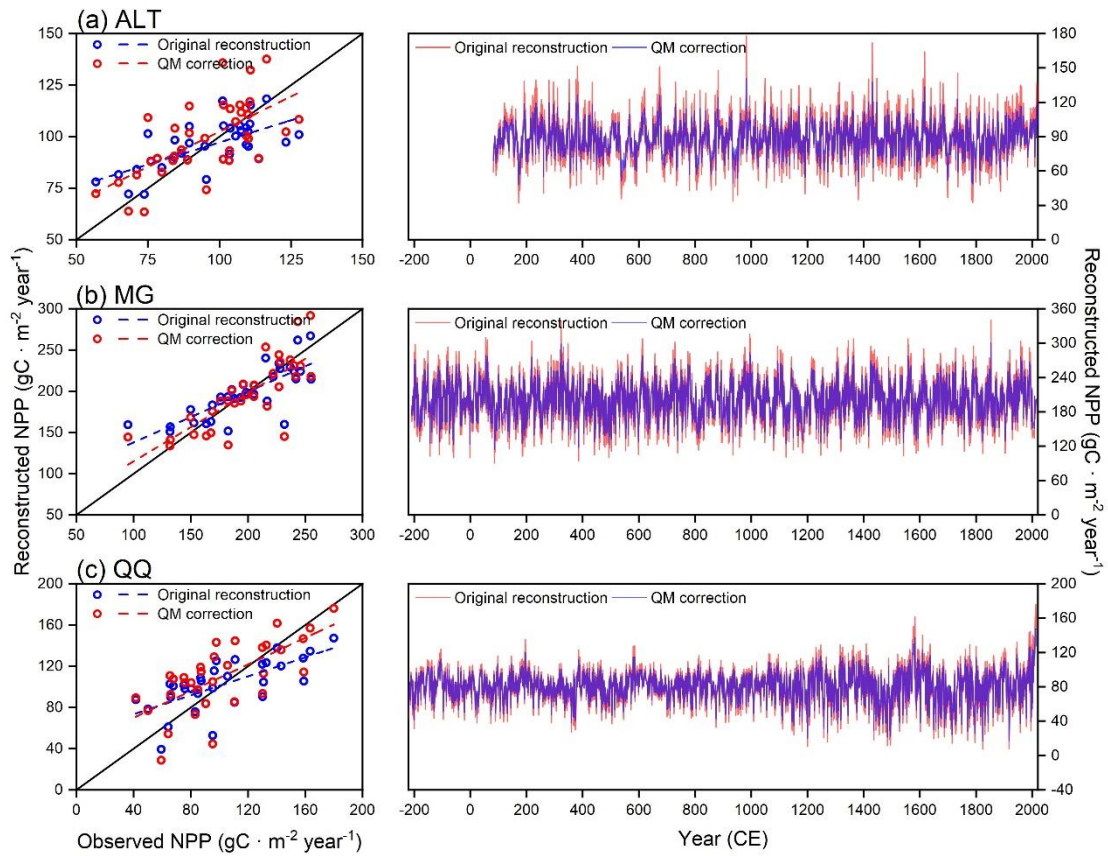


Fig. S4. (a) The 1:1 scatter plot (left) and the comparison of NPP reconstructions (right) before and after bias correction using the quantile mapping (QM) method. (b-c) are same as (a), but for MG and QQ, respectively.

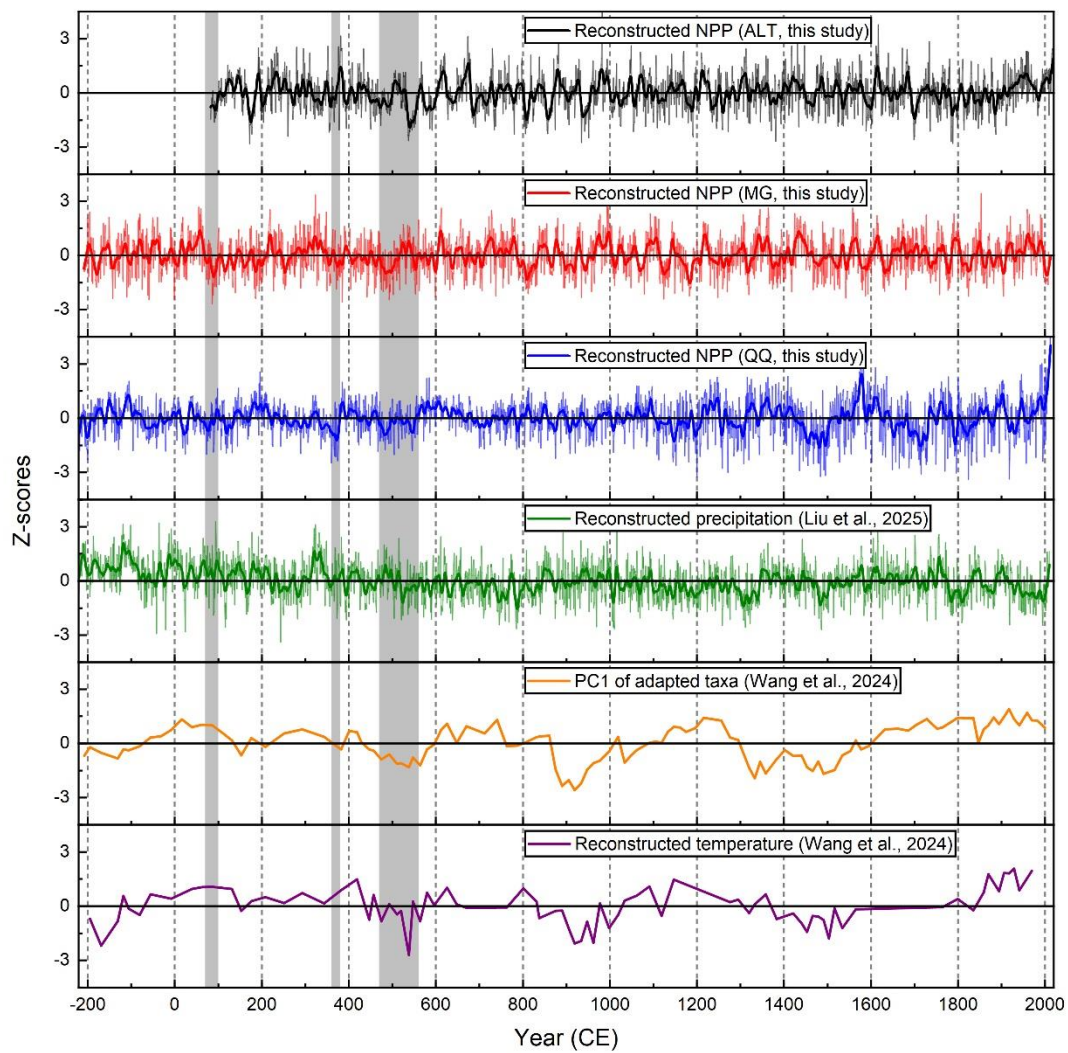


Fig. S5. NPP reconstructions based on tree-ring widths from this study, precipitation reconstruction based on tree-ring oxygen isotopes from Liu et al. (2025), PC1 from different chironomid taxa, and reconstructed temperature based on lake sediments from Wang et al. (2024). Three major migration periods (70s–100s, 360s–380s, and 470s–560s) are highlighted in grey shading.

Table S1. Sampling site information.

Region	Site	Latitude	Longitude	Altitude	Period	Species
Altai Mountains	mong016	48.6	88.37	/	1469–2004	<i>Larix sibirica</i>
	mong020	48.27	88.87	/	1537–2005	<i>Larix sibirica</i>
	mong024	48.5	88.5	/	1215–2004	<i>Larix sibirica</i>
	mong025	48.7	88.8	/	1565–2004	<i>Larix sibirica</i>
	russ246	47.5	87.5	/	-359–2011	<i>Larix sibirica</i>
	ZLS	46.72	90.95	2425	1563–2019	<i>Larix sibirica</i>
	DKL1	48.14	88.34	2332	1170–2019	<i>Larix sibirica</i>
	DKL2	48.14	88.36	2282	1221–2019	<i>Larix sibirica</i>
Mongolia	mong041	48.17	99.87	2060	-732–2014	<i>Pinus sibirica</i>
	mong042	46.68	101.77	2125	-416–2013	<i>Pinus sibirica</i>
Qilian Mountains	chin005	37	98.5	3800	840–1993	<i>Juniperus przewalskii</i>
	chin052	37.45	97.54	3920	404–2002	<i>Juniperus przewalskii</i>
	chin054	37.45	97.79	3700	711–2003	<i>Juniperus przewalskii</i>
	chin055	37.51	97.06	3780	1237–2002	<i>Juniperus przewalskii</i>
	chin061	37.03	98.63	3700	857–2003	<i>Juniperus przewalskii</i>
	chin069	36.95	98.55	/	-1495–808	<i>Juniperus przewalskii</i>
	chin070	38.57	99.33	/	56–2009	<i>Juniperus przewalskii</i>
	YQ	39.61	97.88	3100- 3500	134–1140	<i>Juniperus przewalskii</i>
	CHN	37	98.74	3588	1708–2013	<i>Juniperus przewalskii</i>

Table S2. Leave-one-out cross-validation statistics for the NPP reconstructions.

	r	RE	PMT	Sign test
ALT (1982-2018)	0.610**	0.370**	6.204**	26 ⁺ /11*
MG (1982-2013)	0.784**	0.375**	4.475**	27 ⁺ /5***
QQ (1982-2013)	0.622**	0.381**	4.789**	23 ⁺ /9***

*, **: Significant at $p < 0.05$, $p < 0.01$.

Table S3. Comparisons with important historical events related to the migration of nomadic peoples in Inner Eurasia.

Event	NPP anomaly (%)	Consecutive 2+ years below a standard deviation (%)
Xiongnu occupied Qilian Mountain and forced the Yuezhi to migrate westward	190–170 BC: -12.2% (MG)	182–179 BC: -23.1%–35.9% (MG)
Han Dynasty expelled the Xiongnu and occupied the Hexi Corridor	134–123 BC: -7.4% (QQ)	120–119 BC: -25.8%–29.4% (MG)
Eastern Han defeated the Northern Xiongnu and forced them to migrate westward	69–101 CE: -9.8% (MG)	86–88 CE: -31.6%–54.8% (MG)
	82–101 CE: -15.0% (ALT)	91–92 CE: -20.6%–35.1% (MG)
	58–92 CE: -9.8% (QQ)	
Xiongnu migrated southward deep into Han Empire territories	105–125 CE: -8.0% (MG)	185–187 CE: -28.3%–48.7% (MG)
	129–142 CE: -9.2% (MG)	171–174 CE: -30.8%–63.7% (ALT)
	154–171 CE: -9.6% (MG)	176–178 CE: -36.1%–51.3% (ALT)
	180–211 CE: -8.8% (MG)	
Upheaval of the Five Barbarians	166–185 CE: -23.3% (ALT)	
	256–312 CE: -8.5% (QQ)	366–367 CE: -45.2%–55.7% (QQ)
	331–379 CE: -17.2% (QQ)	369–370 CE: -36.2%–57.0% (QQ)
Nomadic peoples continue to migrate to northern China and Europe	368–388 CE: -9.4% (MG)	372–376 CE: -33.4%–62.8% (QQ)
		356–358 CE: -21.6%–34.1% (MG)
	403–420 CE: -5.5% (MG)	484–486 CE: -21.3%–38.5% (MG)
	427–447 CE: -6.2% (MG)	493–495 CE: -33.0%–50.0% (MG)
Replacement of the Rouran by the Türks, and Avars reach Black Sea	455–468 CE: -6.8% (MG)	500–502 CE: -24.7%–44.4% (MG)
	470–516 CE: -12.2% (MG)	
	531–561 CE: -27.0% (ALT)	551–553 CE: -27.5%–43.8% (MG)
Division of the Turkic Empire into the Western and the Eastern Empires	512–553 CE: -8.7% (QQ)	555–556 CE: -24.5%–32.7% (MG)
	548–559 CE: -11.1% (MG)	
Fall of the Eastern Turkic and Xueyantuo Khanates	570–602 CE: -16.6% (ALT)	580–581 CE: -24.1%–25.2% (MG)
	577–588 CE: -8.1% (MG)	578–581 CE: -23.2%–27.9% (ALT)
Decline of the Uighur Khanate	632–643 CE: -13.1% (MG)	627–628 CE: -25.0%–33.5% (ALT)
	626–647 CE: -9.6% (ALT)	
Chaotic period before Genghis Khan unified Mongolia	787–834 CE: -14.1% (MG)	799–800 CE: -24.5%–26.4% (MG)
		807–810 CE: -32.6%–38.4% (MG)
	1158–1210 CE: -11.5% (MG)	1180–1186 CE: -27.4%–45.8% (MG)
	1174–1194 CE: -15.8% (ALT)	1189–1190 CE: -26.9%–27.5% (MG)
	1103–1135 CE: -6.6% (QQ)	1181–1183 CE: -30.3%–64.6% (QQ)
	1186–1187 CE: -24.2%–34.8% (ALT)	
	1190–1191 CE: -51.7%–54.9% (ALT)	